Self-sustainable Sensor Networks with Multi-source Energy Harvesting and Wireless Charging

Pengzhan Zhou[1], Cong Wang[2], and Yuanyuan Yang [1]

[1]*Dept. of Electrical and Computer Engineering, Stony Brook University, Stony Brook, NY 11794, USA*
[2]*Dept. of Computer Science, Old Dominion University, VA 23529, USA*

Abstract—**Energy supply remains to be a major bottleneck in Wireless Sensor Networks (WSNs). A self-sustainable network operates without battery replacement. Recent efforts employ multi-source energy harvesting to power sensors with ambient energy. Meanwhile, wireless charging is considered in WSNs as a reliable energy source. It motivates us to integrate both fields of research to build a self-sustainable network and guarantee operation under any weather condition. We propose a three-step solution to optimize this new framework. We first solve the Sensor Composition Problem (SCP) to derive the percentage of different types of sensors. Then we enable self-sustainability by bringing energy harvesting storage to the field for charging the Mobile Charger (MC). Next, we propose a 3-factor approximation algorithm to schedule sensor charging and energy replenishment of MC. Our extensive simulation results demonstrate significant improvement of network lifetime and reduction of network cost. The network lifetime can be extended at least three times compared with traditional approaches and the charging capability of MC increases at least 100%.**

Index Terms—**Multi-source energy harvesting, wireless charging, wireless sensor networks, energy self-sustainable**

I. INTRODUCTION

The research of energy efficiency in wireless sensor networks (WSNs) has mainly focused on energy conservation such as low-cost communication, duty cycling, adaptive control and MAC/routing protocols [1]–[3]. These studies improve energy efficiency but yet to solve the fundamental problem of energy provisioning. Sensors will deplete energy ultimately and battery replacement is necessary but infeasible for large networks. Energy harvesters can acquire energy from the environment, e.g., solar, wind, vibration, thermal, and electromagnetic radiation [4]–[6], and made commensurate to sensor size. Unfortunately, ambient source is dynamic, and constant interruption of power supply is expected (e.g., solar harvesting during cloudy/raining days). Thus, new solutions combine multiple sources together to improve system robustness (e.g., solar-wind system [7]). However, under extreme weather conditions, it may still suffer from energy shortage when none of them are available. To this end, we introduce wireless charging as a backup and reliable energy source [8], [9]. Due to limited charging range, a Mobile Charger (MC) is usually employed to approach the proximity of sensors for effective charging [10].

Previous work studied energy efficiency for WSNs from different network layers [11] to system/application level optimizations [12]. However, the success of these mechanisms cannot escape from the fundamental problem of energy supply. For energy harvesting, researchers developed low-cost solar panels and wind turbines of compact sizes [7], [18], [19]. They also utilized MCs for charging sensors wirelessly. Nevertheless, these systems are barely scalable since the MCs have to visit each sensor one by one [13]. To overcome the drawbacks of both approaches, in this paper, we combine multi-source energy harvesting and wireless charging to realize energy self-sustainability in large-scale WSNs that require continuous sensing, coverage and reporting.

The main challenge is due to the inherent dynamics in ambient energy. Solar and wind energy are both subject to micro-climate variation that fluctuates rapidly due to spatial-temporal factors. For instance, cloud movements, sunlight angle, foliage shades, building obstructions, temperature and humidity all have impacts on the harvested energy. During rainy days, solar irradiance is limited; in hot and humid season, wind could completely stop for days. Thus, it is critical for the system to be cognizant of the spatial and temporal characteristics of the weather, and plan sensing, data processing, and communication accordingly. Energy-harvesting sensors are still not enough to guarantee robustness because 1) none of the energy sources may be available in case of extreme weather, 2) nonuniform energy distribution may cause network disruption. To this end, it is essential to provide a backup energy source as wireless charging is employed to support sensors for sensing and relaying data.

To make the system fully autonomous and self-sustainable, the MC needs to replenish its own energy. Most of the previous work redirects the MC back to the base station with connection to the power grid [15]. However, such infrastructure could be unavailable in ad-hoc applications such as wildlife and pollution monitoring. To this end, we deploy a few devices called *Energy Harvesting Base Stations* (EHBS) to harvest and store enough energy with large device. When the MC depletes its energy, it recharges its own battery at EHBS so the network no longer relies on electricity from the power grid.

The new framework poses a series of new challenges. First, how to determine the optimal combination of sensors harvesting different energy, regarding the energy profiles (called *sensor composition problem*)? Second, where to deploy EHBS to maximize energy output while minimizing moving cost of the MC? Third, how to schedule activities of the MC to respond charging requests and replenish its own battery at EHBS? We build a suite of algorithms to answer these questions in a systematic manner. First, we find that the sensor composition problem can be solved optimally in polynomial time by network flow [21]. Second, we propose an algorithm that can partition sensing fields into similar regions. Then we deploy EHBS by jointly considering potential moving cost of the MC and spatial-temporal energy distributions. Finally, we formulate the scheduling problem into a variant of the *Interval Schedule Problem* [25], and propose a greedy and 3-factor
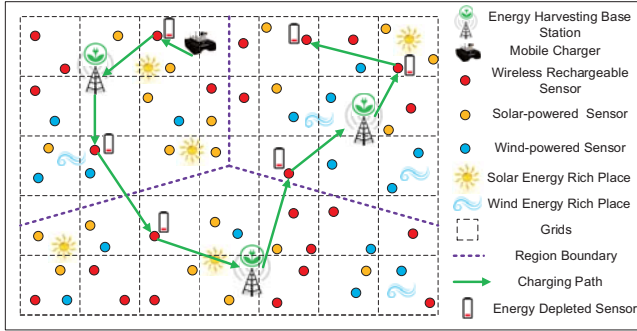
approximation algorithms.

Fig. 1. An overview of multi-source energy harvesting and wireless charging WSN integrated with EHBS.

The contributions of this paper are summarized below. First, we find the optimal combination of sensors for diverse energy profiles and minimize deploying cost. Second, we study the optimal placement of EHBS to achieve the maximal energy output and optimal sensor coverage. Third, we propose a 3-approximation algorithm to plan MC's activity by jointly considering sensor charging and its own energy replenishment. Finally, we conduct extensive simulations to evaluate the performance of the new framework and compare with the previous work. Our results indicate that the proposed framework extends the network lifetime by three times and doubles the charging capability of MC. To the best of our knowledge, this is the first work that jointly considers multi-source energy harvesting with wireless charging to enable a self-sustainable WSN.

The rest of the paper is organized as follows. Section II presents the network model and assumptions. Section III formulates the optimal sensor composition problem. Section IV investigates the optimal deployment of EHBS considering energy output and coverage of sensors. Section V studies the scheduling of MC's activities to achieve the best coverage of different grids. Section VI evaluates the performance of the network and Section VII concludes the paper.

II. PRELIMINARY

This section describes the network model and an overview of the architecture. Important notations used in this paper are summarized in Table I.

A. Network Model and Assumptions

Fig. 1 gives an example of a field divided into 3 regions, where one EHBS is deployed for each region. The ideal setting is to equip each sensor with all kinds of harvesting devices, at a high cost of system complexity and risk to break down. To mitigate these, we assume each sensor is equipped with either one energy harvesting device (e.g., solar or wind), or wireless charging coils. Although it may not fully utilize the environmental energy, the proposed solution is more cost-effective for large networks and different types of sensors can be deployed interchangeably to adapt the local energy distribution. We assume the micro-climate data is available.

TABLE I
LIST OF IMPORTANT NOTATIONS

Notation	Definition
y_{uv}	Grid in the u-th row and v-th column
n_{uv}	Number of sensors in y_{uv}
η_z^{uv}	Percentage of z-th type sensors in y_{uv}
c_z	Manufacturing cost of one z-th type sensor
t_k	k-th time slot
q	Number of EHBS
$\mathcal{G}_l$	l-th region
a	Region-size precision index
ξ	Size deviation ratio
x_i	i-th charging request

In practice, it is easy to obtain via driving the MC around for a preliminary field survey. Solar and wind-powered sensors are deployed according to the energy distribution, with higher density at energy-rich locations. Wireless rechargeable sensors are deployed at the same time with other energy harvestable sensors considering the energy profiles.

B. Overview of Framework

The solution begins with finding the appropriate proportions of sensors to satisfy the task and energy demands. According to the density of sensors and deployment patterns, EHBS are placed at strategic locations to minimize potential moving cost of the MC. With the locations of EHBS, the MC schedules its activity of charging sensors and returns to EHBS for the battery refill. The first problem aims to minimize the fixed cost of a network plan. The second one attempts to reduce operating cost and enhance energy-efficiency. The third one makes sure the network operates without disruption. Although the three objectives look different, they share the same goal to optimize the overall design and cost of the network.

We admit that a global, cross-layer optimization that combines all these goals is more comprehensive. However, the inter-dependence between these objectives would definitely complicate the solution space and system design. For example, the deployment of EHBS relies on the density of surrounding sensors/their types, which is, in turn, solved by the sensor composition problem at first. If the two problems are considered together, the solution space would increase many-fold, and make the problem impractical to solve. As a result, we pursue a three-step approach following a logic and systematic manner discussed next.

III. SENSOR COMPOSITION PROBLEM

In this section, we study the *Sensor Composition Problem* (SCP). The composition of sensors defines their ratio at various locations depending on the energy sources/income (e.g., solar, wind, and wireless charging). Different types of sensors usually have diverse manufacturing costs, e.g., solar panels are more expensive than wireless charging coils and wind turbines. The objective of SCP is to minimize the total cost of sensors while making sure network energy is sufficient to support sensor activity. The inputs are the energy distributions. Sensors work together in the network to tackle different tasks such as sensing, computing and communication.

To facilitate analysis, the sensing field is divided into grids. y_{uv} represents the coordinate of the grid region in the u-th

row and v-th column. n_{uv} is the number of sensors to be deployed in the grid y_{uv}. We consider l types of sensors ($l = 3$), where the percentages of each type of sensors are, η_1^{uv} for solar, η_2^{uv} for wind and η_3^{uv} for wireless-powered sensors. The formulation here is general for any l, i.e., l can be more than 3 depending on the number of available energy sources. $p_z(y_{uv}, t_k)$ is the power income from the z-th energy source at location y_{uv} and time t_k. The grid partitions the field with minimum granularity, e.g., 100m × 100m, so energy distribution is approximately uniform in each grid. Let $C(y_{uv}, t_k)$ denote the required energy at location y_{uv} at time t_k, composed of sensing, computing, communication and data transmission. The sufficient condition for the network to maintain operation is to ensure the sum of energy income is not less than the energy consumed at any arbitrary time,

$$\sum_{z=1}^{l} n_{uv}\eta_z^{uv} p_z(y_{uv}, t_k) \geq C(y_{uv}, t_k), \forall u, v, k. \quad (1)$$

To find the optimal composition of sensors while maintaining energy balance, we formulate SCP into the *network flow problem*, which finds the feasible flows meeting the demands of the sink, and involves the least cost from the sensor nodes. As shown in Fig. 2, the *Source* represents all kinds of energy income, and the *Sink* represents all energy consumption tasks. There are a total of n sensors and m tasks, where the index of sensors and tasks are denoted by i and j separately. The sensors are represented by the nodes directly connected with the source and the tasks are represented by the nodes directly connected with the sink in Fig. 2. The m tasks include sensing, computing and data transmission in different grids y_{uv}. If sensor i can complete the task j, then a link exists between them in the flow graph. In the grid y_{uv}, the flow of the link is denoted as x_{ijz}^{uv} (z denotes the sensor type). The energy consumption of task j is E_j^{uv}. The optimization problem can be formulated as Eqs. (2) to (5),

$$\textbf{P1:} \quad \min \sum_{z=1}^{l} n_{uv}\eta_z^{uv} c_z, \quad (2)$$

$$\textbf{s.t.} \sum_j x_{ijz}^{uv} \leq p_z(y_{uv}, t_k), \forall\, i, k, z \quad (3)$$

$$0 \leq x_{ijz}^{uv} \leq p_z(y_{uv}, t_k), \forall\, i, j, k, z \quad (4)$$

$$\sum_i x_{ij}^{uv} \geq E_j^{uv}(t_k), \forall\, j, k. \quad (5)$$

Eq. (2) minimizes the total manufacturing costs composed of $l = 3$ types of sensors, where c_z is the cost of deploying one z-th type sensor. Eq. (3) ensures all the tasks conducted on sensor i of type z do not consume more energy than the harvested energy $p_z(y_{uv}, t_k)$ at any time t_k. Eq. (4) ensures that the energy consumed in each link must be positive and not larger than the harvested energy $p_z(y_{uv}, t_k)$. Eq. (5) ensures that the energy being assigned to complete task j is more than its energy requirement $E_j^{uv}(t_k)$. $p_z(y_{uv}, t_k)$ can be derived from the historical data or offline survey conducted by the MC. A day is slotted into equal intervals t_k. The problem solves for each grid y_{uv} in the field. For given n_{uv} and η_z^{uv}, **P1** is
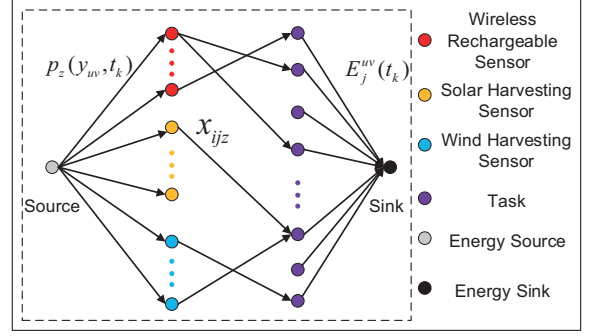

Fig. 2. Formulation of SCP into a network flow problem.

a *maximum flow problem*, which can be optimally solved by *MPM* algorithm [21]. By plugging different values of n_{uv} and $\eta_z^{(uv)}$, we can find the values with minimum cost according to Eq. (2), which has a feasible solution for the problem. For each computation, MPM algorithm takes $\mathcal{O}((n + m)^3)$ time. For the number of sensors n, $\binom{n+2}{2}$ number of combinations are tested, which is in the order of $\mathcal{O}(n^2)$, so the total time complexity is $\mathcal{O}((n + m)^3 n^2)$.

IV. DEPLOYMENT OF ENERGY HARVESTING BASE STATION

An indispensable part of the framework is the wireless rechargeable sensors. The MC serves as a carrier to deliver energy from the base station to the sensors. Previous research assumes this base station is in the vicinity of the power grid. Unfortunately, it is not only sub-optimal for the MC (in terms of higher moving cost), but also limited in ad-hoc environment with no access to the power infrastructure. To address this problem, multiple Energy Harvesting Base Stations (EHBS) are adopted in this paper. The EHBS is a simple device with two major components: a large capacity battery and solar-wind harvesting device. They can harvest different kinds of energy at the same time and store enough energy to the battery. The total energy harvested by the EHBS should be much larger than the energy consumption in the network for self-sustainability as estimated during the initial network planning. The harvesting device is large enough to generate enough energy. EHBS also offers a wireless charging interface to transmit energy to the MC. When the MC depletes its own energy, it visits the nearest EHBS for recharging.

We study the deployment problem of EHBS. The locations of EHBS determine the amount of energy they can harvest and the moving cost of MC to reach them. The goal is to find locations that are energy-rich and easily accessible by the MC. The energy-rich locations can be found from historical data. In addition to energy income, EHBS should be deployed close to places with more energy demands, so as to reduce moving cost of the MC. Therefore, both energy distribution and charging demands from MC should be jointly considered.

A. Division of Sensing Field

After the initial survey and estimation, assume there are q EHBS to be deployed that satisfy the energy demands.

Algorithm 1: Field division algorithm

1 **Input**: Number of regions q, precision index a, the field.
2 **Output**: q regions $\{\mathcal{G}_l\}$ dividing the field.
3 $k \leftarrow \lceil a\sqrt{q} \rceil$; divide field into k^2 grids $\{y_{uv}\}$, $\mathcal{Y} \leftarrow \{y_{uv}\}$.
   $T \leftarrow \{y_{uv} : \underset{y_{uv} \in \mathcal{Y}, \forall u}{\arg\min}\{v\}\}$, $L \leftarrow \{y_{uv} : \underset{y_{uv} \in \mathcal{Y}, \forall v}{\arg\min}\{u\}\}$, $l \leftarrow 1$.
4 $y_{ij} = \underset{y_{uv} \in T}{\arg\min}\{u\}$.
5 **if** $y_{i(j+a-1)} \in \mathcal{Y}$ **then**
6 $\quad$ $\mathcal{G}_l \leftarrow \{y_{uv} : i \le u \le i+a-1, j \le v \le j+a-1\}$,
   $\quad$ $\mathcal{Y} \leftarrow \mathcal{Y} \setminus \mathcal{G}_l$, $l \leftarrow l+1$, $T \leftarrow \{y_{uv} : \underset{y_{uv} \in \mathcal{Y}, \forall u}{\arg\min}\{v\}\}$,
7 $\quad$ **jump** to **line 4**
8 $y_{ij} = \underset{y_{uv} \in L}{\arg\min}\{v\}$.
9 **if** $y_{i(j+a-1)} \in \mathcal{Y}$ *And* $y_{(i+a-1)j} \in \mathcal{Y}$ **then**
10 $\quad$ **jump** to **line 4**
11 **while** $|\mathcal{Y}| > k^2 - (a-1)q$ **do**
12 $\quad$ **while** $|\mathcal{G}_l| < a^2$ **do**
13 $\quad\quad$ $\mathcal{G}_l \leftarrow \mathcal{G}_l \bigcup \{y_{ij}\}$, $\mathcal{Y} \leftarrow \mathcal{Y} \setminus \{\mathcal{G}_l\}$,
   $\quad\quad$ $T \leftarrow \{y_{uv} : \underset{y_{uv} \in \mathcal{Y}, \forall u}{\arg\min}\{v\}\}$, $y_{ij} = \underset{y_{uv} \in T}{\arg\min}\{u\}$.
14 $\quad$ $l \leftarrow l+1$.
15 $\quad$ **while** $|\mathcal{G}_l| < a^2$ **do**
16 $\quad\quad$ $\mathcal{G}_l \leftarrow \mathcal{G}_l \bigcup \{y_{ij}\}$, $\mathcal{Y} \leftarrow \mathcal{Y} \setminus \{\mathcal{G}_l\}$,
   $\quad\quad$ $L \leftarrow \{y_{uv} : \underset{y_{uv} \in \mathcal{Y}, \forall v}{\arg\min}\{u\}\}$, $y_{ij} = \underset{y_{uv} \in L}{\arg\min}\{v\}$.
17 $l \leftarrow l+1$, $\mathcal{G}_l \leftarrow \mathcal{Y}$.

To deploy the EHBS, the field is divided into q similar-size regions represented by $\{\mathcal{G}_l\}$. Since EHBS have similar output power, deploying them to regions of similar size can minimize the variance of energy between different regions. This way, the network can avoid coverage holes due to energy depletion from the entire region. One EHBS is deployed for each region with the best coverage. In this subsection, the method to divide the field is studied.

There are some trivial ways to divide the field. Take a square area for instance, it can be conveniently split into q equivalent rectangles. However, this method has some drawbacks: 1) nonuniform traveling distance in each rectangle. The distance from the center of the rectangle to the edge varies according to the directions emitted from the center. Traveling distance of the MC from sensors to the EHBS is unbalanced, which causes charging delay to those sensors far from the EHBS 2) Uneven locations of EHBS (centroid of the rectangles). Their locations tend to concentrate near the center of the square, that leads to inconvenient access to the nodes on the boundaries. Comparing one circle region and one rectangular region of the same area, there are more sensors in the rectangular regions whose distances from the centroid are even larger than the maximum distance (i.e. the radius) in the circle region. It can be proved that, among different shapes of regions, circular area has the minimal total distance (i.e. summation of distance from any point in the region to the centroid). Based on these observations, the strategy should generate regions as isotropic as possible (e.g., square, since square is the circle for grids) of similar sizes. To our best knowledge, there are few previous research discussing the method to divide field of any shape into q similar-size and isotropic regions.
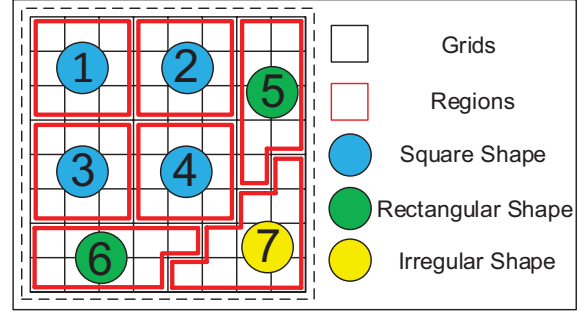

Fig. 3. Division of 8×8 square field into 7 regions.

We propose a new algorithm to generate q such regions, that can be applied to any shape. Take a square field for instance, we divide it into k^2 equal-size square grids. k is derived as $k = \lceil a\sqrt{q} \rceil$, where a is an input integer called precision index. Large a results finer granularity. Then the side length for most of the smaller square region is derived according to $\lfloor k/\sqrt{q} \rfloor = \lfloor \lceil a \cdot \sqrt{q} \rceil / \sqrt{q} \rfloor$. This means that for most of the small square regions, the side length is $\lfloor k/\sqrt{q} \rfloor$ times the grid length, and each square region contains $\lfloor k/\sqrt{q} \rfloor^2$ grids. Thus, we have $\lfloor \frac{k}{\sqrt{q}} \rfloor = a$.

Next, the square field is divided into q regions. Starting from the grid on the top left corner of the field, the algorithm goes to the right by a grids, and goes downward by a grids, and generates a square region, which contains a^2 grids. This square region is the first one for EHBS. Then, the next region is derived by going further to the right, which is adjacent to the previous square region. The process repeats until there is no more complete square region found on the right hand side. Then the process continues downward until there is no more complete square region for the entire field. For the remaining grids, starting from the grid on the bottom left corner of the field, the first a^2 adjacent grids form another region. The same process also starts from the top right corner. This process continues until the number of the remaining unassigned grids falls within the interval between $[a^2, 2a^2-1]$. Finally, the remaining grids form the last region. The algorithm is summarized in Algorithm 1.

The algorithm produces most regions in square shape, some rectangles, and at most one with irregular shape. For quantitative evaluation, we further define an index ξ called *Size Deviation Ratio* as the ratio between the difference of largest and smallest region size and the mean,

$$\xi = \frac{\text{Max} - \text{Min}}{\text{Mean}}. \qquad (6)$$

For the example of square field (grid area has unit 1), Min $= a^2$, and Max $= \lceil a\sqrt{q} \rceil^2 - (q-1)a^2$, and Average $= \lceil a\sqrt{q} \rceil^2/q$. Hence, ξ is,

$$\xi = q - \frac{a^2 q^2}{\lceil a\sqrt{q} \rceil^2}. \qquad (7)$$

Fig. 3 gives an example of the algorithm. The field is divided into 7 regions. $a = 3$, so the field contains 8×8 grids. The number represents the order of the region being

generated. The first 4 regions are squares. The next two regions have rectangular shape, and region $\mathcal{G}_7$ contains the remaining unassigned grids. Note that the regions derived by the algorithm have comparable sizes. The size deviation ratio is 11% for this example.

B. Deployment of EHBS

Next, EHBS are ready to be deployed into the q regions. Described in Section III, the total amount and percentages of different sensors are determined independently for each grid y_{uv}, thus the density ρ_{uv} of wireless rechargeable sensors in grid y_{uv} is also inhomogeneous for each grid. Using the centroid can achieve the largest coverage of the sensor groups in each grid [22] as well as balance the charging latency to reach those nodes from the centroid. For region $\mathcal{G}_l$, its centroid C_l by considering the grids contained in $\mathcal{G}_l$ is $C_l = \sum_{(u,v) \in \mathcal{G}_l} y_{uv} \rho_{uv} / \sum_{(u,v) \in \mathcal{G}_l} \rho_{uv}$.

The location of EHBS should be close to the centroid C_l and the energy-rich places,

$$\arg\max_x \big(\alpha(e_1(x) + e_2(x)) - ||x - C_l||_2 \big), \forall x \in \mathcal{G}_l, \quad (8)$$

where $e_i(x)$ denotes the expectation of the i-th type energy at location x (from historical energy profile). $||x - C_l||_2$ is the MC's moving cost between x and C_l (in proportion to the Euclidean distance). α is a scaling parameter to balance the two. The optimal location x^* in region $\mathcal{G}_l$ that maximizes the sum of Eq. (8) is selected as the location of the EHBS. It jointly considers the potential moving cost and energy distribution to maximize energy efficiency. The parameter α is a user-input of the network, which reflects the importance of these two components. α can be raised if the power of the harvested energy is more important for the user; otherwise, α can be cut back if saving of the traveling cost is more crucial. Due to the uneven distribution of the harvestable energy, it is very difficult to represent the harvestable energy in a function format. The region can be divided into some candidate locations according to the requirement of the granularity. To solve Eq. (8), we can enumerate these locations as the inputs, and pick the one with the largest output as x^*. With the certain granularity of the candidate location, this method is scalable, and the complexity of the method is in the order of $\mathcal{O}(S)$, where S is the area of the field.

V. Scheduling Sensor Charging and Battery Replenishment for Mobile Charger

The MC charges sensors to satisfy their energy demands as well as replenishes its own energy at the EHBS once the energy is depleted. This section studies scheduling of such activities.

A. Group Interval Scheduling Maximization

Charging requests from sensors are from various locations in the field due to dynamic spatial-temporal energy distribution. Wireless rechargeable sensors play a key role in this situation to maintain network operation. The objective of the MC is to satisfy as many requests as possible in each grid, while also
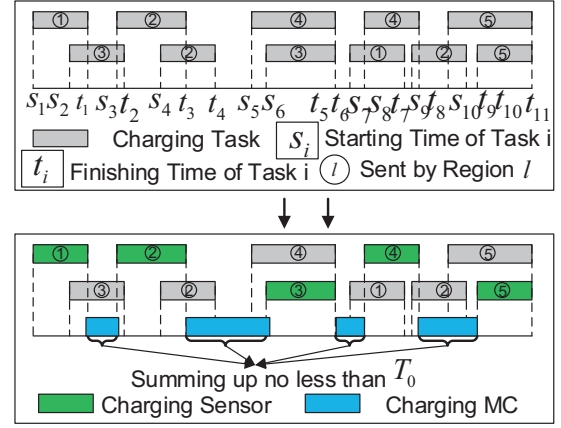

Fig. 4. Joint scheduling of sensor charging and energy replenishing by MC.

satisfying energy demands from other grids. In the meanwhile, the MC should determine an appropriate time to replenish its own battery at EHBS. The charging requests are classified by the grids that are sending them.

Energy requests arrive at the MC at different time during time T. A charging task x_i starts at time s_i and ends at t_i. Meanwhile, the MC needs to spend T_0 time to refill its own battery in T. We ignore the traveling time of MC because it takes much less compared to the charging time. For example, moving on a 10×10 region with a speed of 10 m/min results 1.5 min on the longest diagonal movement. Compared to that battery charging usually takes 30-90 mins, such minimum time expense is ignored to simplify the problem. As shown in Fig. 4, schedule of charging tasks may have temporal conflict with each other. Due to limited wireless charging range, the MC can only respond to one request at a time. To charge as many groups as possible, during T time, the MC finds the maximum number of grids containing non-conflicting charging tasks and leaves at least T_0 time for recharge. The problem is formulated as follows,

$$\textbf{P2:} \ \max |\mathcal{A}|, \quad (9)$$

$$\textbf{s.t.} \ T_0 \cdot P_r \geq \sum_{i \in \mathcal{A}} (t_i - s_i) \cdot P_c - E_{mc}, \quad (10)$$

$$T_0 + \sum_{i \in \mathcal{A}} (t_i - s_i) \leq T. \quad (11)$$

$\mathcal{A}$ is the set of grids selected by the MC for charging. P_r and P_c are the charging rates at EHBS and sensors, repectively. E_{mc} is the residual energy of the MC. **P2** maximizes the number of grids to be charged in T, while constraint (10) ensures the energy replenished to the MC is larger than the energy demand of sensors, and constraint (11) imposes the time spent on charging sensors and recharge time is within T.

The optimization problem is a variation of *Group Interval Scheduling Problem* (GISP) [23]. It considers groups of tasks, where each task x_i is represented by an interval indicating its starting time s_i and finishing time t_i. A subset of all the intervals are considered to be compatible if any two of them do not have any overlapping with each other. If an interval is

chosen, then it is the representative of the group containing it. GISP aims to find the subset of compatible intervals with the maximum coverage of different groups, i.e., maximize the number of groups (grids) having at least one representative in the derived subset.

Different from GISP, **P2** leaves T_0 in addition to the charging tasks. The constraints (10) and (11) give the upper and lower bound for T_0. Combining them gives the following constraint,

$$\sum_{i \in \mathcal{A}} (t_i - s_i) \leq \frac{T + E_{MC}/P_r}{1 + P_c/P_r}. \quad (12)$$

Therefore, if the summation of compatible intervals of different charging tasks is not larger than the r.h.s of Eq. (12), then it is a feasible solution for **P2**. The new problem is an extension to GISP and we call it *Reserved Group Interval Scheduling Problem* (R-GISP).

Definition. *Reserved Group Interval Scheduling Problem* (R-GISP) looks for the a set of non-overlapping representatives of maximum sizes from groups of intervals and assures the summation of the lengths of all intervals in the set is no larger than a given constant.

NP-Hardness. *R-GISP is NP-hard.*

Proof: In order to prove R-GISP is NP-hard, we first prove GISP is NP-hard and GISP can be reduced to R-GISP. *A special case of GISP is NP-hard.* A special case of GISP solves the problem whether there is such compatible set that contains at least one representative from each group, i.e., the size of the groups being represented is equal to the number of groups. This special case is called *Group Interval Scheduling Decision Problem* (GISDP). It has been proved in [24] that GISDP is NP-hard since *Boolean Satisfiability Problem* is a special case of GISDP and Boolean Satisfiability Problem is NP-hard. GISDP is a special case of GISP where the maximum groups being represented is equal to the total number of groups so GISP is NP-hard. R-GISP removes constraint (12) from GISP so GISP is a special case to R-GISP thus R-GISP is NP-hard. ∎

B. Earliest Finishing First Algorithm

Due to the NP-hardness of R-GISP, it is not possible to find an optimal solution in polynomial time unless P=NP. Hence, we seek sub-optimal solutions in polynomial time.

As shown in Algorithm 2, the charging task x_i with the earliest deadline t_i is chosen. All charging tasks intersecting with it are removed. Charging tasks from the same grid are also removed. This process iterates until no task is left. Second, for those intervals chosen after the first step, the algorithm sums them up and compares the summation with $(T + E_{MC}/P_r)/(1 + P_c/P_r)$, which is the maximum charging time. If the summation is smaller than the maximum charging time, it removes all the intervals overlapping with them. For the remaining intervals, the algorithm performs the first step again. If the summation is larger than the maximum charging time, it removes the longest interval from the covering set until the summation of the remaining intervals is not larger than the maximum charging time. In the last step, for a given

---

Algorithm 2: Earliest Finishing First Algorithm

1 **Input**: A number of n charging requests $\mathcal{X} = \{x_i\}$, $x_i = [s_i, t_i]$, distributed in grids $\{y_{uv}\}$, an empty set $\mathcal{A}$.
2 **Output**: Charging and energy replenishment sequence $\mathcal{A}$ for MC.
3 $\widehat{\mathcal{X}} \leftarrow \mathcal{X}$ **while** $\widehat{\mathcal{X}} \neq \phi$ **do**
4      $f = \underset{x_i \in \mathcal{X}}{\arg\min}\{t_i\}$, $x_f \in y_{uv}$, $\mathcal{A} \leftarrow \mathcal{A} \bigcup \{x_f\}$;
     $\widehat{\mathcal{X}} \leftarrow \widehat{\mathcal{X}} \setminus \{\{x_j : x_j \cap x_f \neq \phi, \forall j\} \bigcup \{x_j : x_j \in y_{uv}, \forall j\}\}$.
5 **if** $\sum_{i \in \mathcal{A}} (t_i - s_i) \leq [T + E_{MC}/P_r]/[1 + P_c/P]$ **then**
6      $\mathcal{X} \leftarrow \mathcal{X} \setminus \mathcal{A}$; **jump** to **line 3**.
7 **if** $\sum_{i \in \mathcal{A}} (t_i - s_i) > [T + E_{MC}/P_r]/[1 + P_c/P]$ **then**
8   **while** $\sum_{i \in \mathcal{A}} (t_i - s_i) > \frac{T + E_{MC}/P_r}{1 + P_c/P_r}$ **do**
9          $e \leftarrow \underset{x_i \in \mathcal{A}}{\arg\max}(t_i - s_i)$; $\mathcal{A} \leftarrow \mathcal{A} \setminus \{x_e\}$
10 MC charges sensors following the charging sequence derived in $\mathcal{A}$.
11 MC replenishes its energy at the closest EHBS during spare time.

Algorithm 3: 3-Approx Shortest Interval First Algorithm

1 **Input**: A number of n charging requests $\mathcal{X} = \{x_i\}$, $x_i = [s_i, t_i]$, distributed in grids $\{y_{uv}\}$, an empty set $\mathcal{A}$.
2 **Output**: Charging and energy replenishment sequence $\mathcal{A}$ for MC.
3 **while** $\sum_{\forall x_i \in \mathcal{A}} |t_i - s_i| \leq [T + E_{MC}/P_r]/[1 + P_c/P]$ **do**
4      $x_j \leftarrow \underset{x_i \in \mathcal{X}}{\arg\min} |t_i - s_i|$, $\mathcal{A} \leftarrow \mathcal{A} \bigcup \{x_j\}$
5   **for** $i=1, 2, 3, \ldots, n$ **do**
6   **if** $x_i \cap x_j \neq \phi$ **then**
7              $\mathcal{X} \leftarrow \mathcal{X} \setminus \{x_i\}$.
8 $\mathcal{A} \leftarrow \mathcal{A} \setminus \{\text{the last interval put into } \mathcal{A}\}$.
9 MC charges sensors following the charging sequence derived in $\mathcal{A}$.
10 MC replenishes its energy at the closest EHBS during spare time.

---

period T, MC performs the charging tasks in $\mathcal{A}$ according to the order of the starting time. MC replenishes its own energy at the closest EHBS when idle.

An example is shown in Fig. 4. 11 charging requests from 5 different regions are received. Solving the algorithm yields that 5 requests from different regions are met so as to achieve the best region coverage. T_0 time is left for the energy replenishment of MC.

The complexity of the algorithm is analyzed below. Assume there are n charging requests from m grids. Sorting requires $\mathcal{O}(n \log n)$ time. First, finding the intervals intersecting with the chosen one takes $\mathcal{O}(n)$ time with at most $\mathcal{O}(m)$ times, and removing the intervals takes $O(n)$ time. Therefore, the time complexity for the first step is $O(n \log n) + O(nm)$. For the second part, summing up the intervals and comparing with the maximum charging time takes $O(n)$ time, and this process takes at most m times, therefore $O(nm)$ in total. The procedure is repeated at most n/m times and the total time complexity is $O(n^2(\log n/m + 1))$.

C. 3-Approximation Algorithm

In this section, we propose a new algorithm as shown in Algorithm 3 with 3-approximation ratio for R-GISP. As far as we know, this is the first approximation algorithm with constant ratio for the R-GISP problem. The previous earliest finishing first algorithm does not have a theoretical bound of performance because choosing the tasks with the earliest

finishing time does not consider the duration of tasks at all. Without a performance guarantee, the ratio between the optimal solution and the result derived is unbounded (can be arbitrarily large in the worst case), and we can not either infer any insight about the optimal solution from the results.

Instead of looking for the earliest finishing time, the new algorithm seeks the shortest interval. For a set of tasks, the algorithm picks the one with the shortest duration, and removes the tasks intersecting with the chosen task from the set of tasks. If the total length of chosen tasks is smaller than $(T + E_{mc}/P_r)/(1 + P_c/P_r)$, then continue the process for the remaining set until the largest set of tasks whose total length is smaller than the preset limit $\frac{T + E_{MC}/P_r}{1 + P_c/P_r}$.

Approximation Ratio. The Shortest Interval First Algorithm has 3-factor approximation for R-GISP.

Proof: Denote the optimal solution for R-GISP as OPT, and the solution derived by the algorithm as SIF. The function f maps any interval $I \in OPT$ to an interval in SIF according to the following rule,

$$f(I) = \begin{cases} \mathbf{0}: I, \text{ if } I \in SIF; \\ \mathbf{2}: \text{ Shortest interval in } SIF \text{ intersecting with } I, \\ \quad \text{if } I \notin SIF \text{ and } I \text{ intersects with intervals in } SIF; \\ \mathbf{3}: \text{ The longest interval in } SIF, \text{ if } I \notin SIF \text{ and } I \\ \quad \text{intersects with no interval in SIF.} \end{cases}$$

The above mapping function from OPT to SIF is composed of three cases. For any interval J in SIF, if $J \in OPT$, then there is only one interval in OPT that could be mapped to SIF according to the compatible property of intervals in OPT.

If $J \notin OPT$ but J intersects with intervals in OPT, then there is at most 2 intervals in OPT that could be mapped to J via function $f(I)$. Assume there are 3 such intervals in OPT, then one of the intervals must be totally covered by J, and is also shorter than J, which contradicts the property that J is the shortest interval that intersects with the duration of J.

For the longest interval J_{max} in SIF, some number of intervals in OPT are mapped to it according to the third case of $f(I)$, which do not intersect with any interval in SIF. Note that, such intervals I in OPT must have longer duration than J_{max}, because J_{max} must be smaller than any interval in the task set which does not intersect with SIF; otherwise it is not the shortest interval to be picked that contradicts the procedures defined in SIF. Therefore, the number of such I's in OPT can not be larger than $|SIF|$; otherwise, the duration of all intervals in OPT is larger than the time limit T, which is a contradiction.

For any interval (besides of the longest) in SIF, $f(I)$ maps at most 2 intervals in OPT to it. For the longest interval J_{max} in SIF, $f(I)$ maps at most $|SIF|$ intervals to it. Since any interval in OPT is mapped to an interval in SIF, $|OPT| \leq 3|SIF|$. ∎

At the end, we compute the time complexity of the 3-approximation algorithm. For n charging requests, sorting them, finding the shortest interval and removing the intersect-
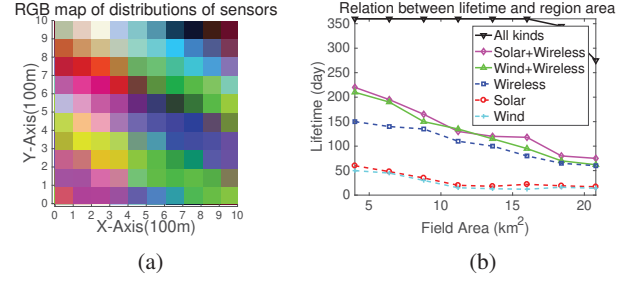

Fig. 5. Optimal sensor composition and network lifetime. (a) RGB map for the best composition of 3 kinds of sensors. (b) Comparison of lifetime for different sensor compositions vs. field sizes.

ing ones take $\mathcal{O}(n \log n)$, and this process is conducted at most n times. The total time complexity is $\mathcal{O}(n^2 \log n)$.

VI. PERFORMANCE EVALUATIONS

We evaluate the performance of the self-sustained framework by a discrete-event simulator developed in MATLAB and compare with the previous work that depends on single energy source [26]. In the simulation, we use data trace of solar radiation from *SOLARGIS* [27] and wind power from *NREL* [28]

The sensing field has side length of $L = 2000$ m. Time is equally slotted (1 hour) and the average energy consumption rate of working sensor is 12 J/min. A typical sensing range r_s is 15 m. Wireless rechargeable sensors have Li-Ion battery of 1200 mAh capacity and 3.7 V working voltage with $\Delta t = 30$ mins charging time from empty to full [14]. Solar/wind-powered sensors have batteries of 2150mAh and 3.7 V working voltage. The manufacturing costs of solar-powered, wind-powered and wireless rechargeable sensors are $50, $35 and $30 for one sensor respectively [16]. The maximum energy harvesting power for solar-powered sensor and wind-powered sensor is 2W·h and 1.5W·h [16] , respectively. The maximum energy harvesting power for EHBS are 2kW·h [17]. The MC moves at a speed of 10 m/min at an energy consumption rate of 5 J/m. When the percentage of remaining energy for wireless rechargeable sensor is lower than a threshold of 20%, they send out requests for recharge. The simulation time is 360 days.

A. Sensor Compositions and Lifetime

First, we evaluate the optimal composition of three types of sensors (solar, wind and wireless rechargeable) for the minimum total cost and evaluate the network lifetime compared with network of one energy source. Fig. 5 (a) demonstrates the number and percentages of 3 kinds of sensors for each grid by applying RGB heatmap. The color of each grid is determined by an $[R \ G \ B]$ vector, where R, G, B represent the solar-powered, wind-powered and wireless rechargeable sensors respectively. The values are proportional to the number of corresponding sensors in each grid, which is normalized by the total number of sensors of their kinds. In other words, the color of each grid is the total number of sensors deployed and the ratios of each kind. For example, when $[1 \ 0 \ 0]$ is red, only solar-powered sensors are deployed in the grid; when $[0 \ 1 \ 1]$ is cyan, the same number of wind-powered sensors
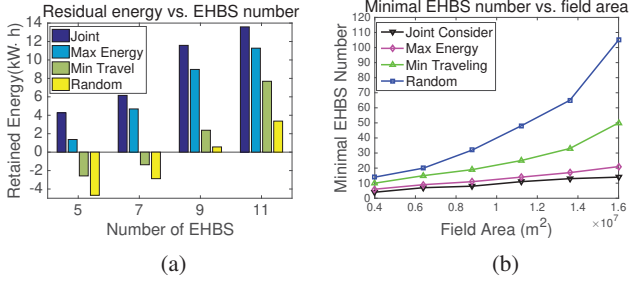
Fig. 6. Residual energy and minimal number of EHBS. (a) Residual energy at each EHBS for different deployment methods. (b) Minimal number of EHBS to achieve energy balance.
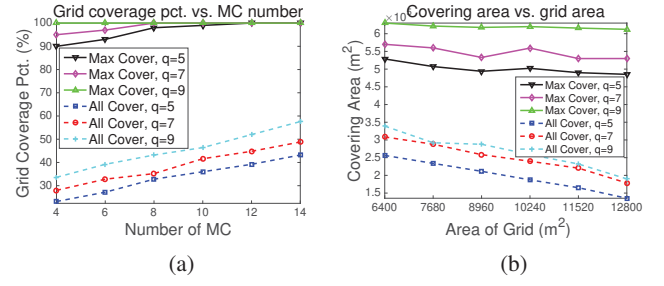

Fig. 7. Grid coverage percentage and covering area by MC. (a) Grid coverage percentage for different covering algorithms. (b) Covering area of one MC for different covering algorithms.

and wireless rechargeable sensors are deployed with no solar-powered sensor.

From Fig. 5(a), it is observed that for the region $[100 \sim 400; 0 \sim 200]$ (i.e., the area in $100m \leq X \leq 400m$ and $0m \leq Y \leq 200m$), similar number of solar sensors and wireless sensors and almost no wind sensors are deployed, since those areas have solar energy whereas lack wind energy; for the region $[100 \sim 400; 600 \sim 800]$, most of the sensors are solar-powered since those areas have abundant solar energy and no wind energy; for the region $[600 \sim 900; 700 \sim 900]$, wind sensors and wireless sensors have similar number while not many solar sensor, since those areas are abundant of wind energy and lacking of solar energy; for the region $[600 \sim 900; 900 \sim 1000]$, there are many sensors of all three kinds, since those areas are lacking of both solar and wind energy; for the region $[0 \sim 300; 900 \sim 1000]$, the numbers of different sensors are similar since those areas are sufficient to provide all kinds of energy. The simulation demonstrates that our framework precisely selects different ratios of sensors reflecting the ambient energy distribution while minimizing the total manufacturing cost.

Fig. 5(b) compares network lifetime, which is defined as the time expansion until the first energy depletion occurs; otherwise, the lifetime lasts the entire simulation time (360 days). Note that some energy depleted nodes would temporarily turn into sleep mode and wait for energy refill from the renewable energy or wireless charging. Other nodes with energy can still execute the network tasks and maintain operation. The simulation is conducted for different sensor compositions. "All kinds" means all three energy sources are used. "Solar+Wireless" means only solar and wireless-powered sensors are used. We alternate through all the combinations and their optimal compositions are computed by the MPM algorithm [21].

The results indicate having all kinds of sensors is able to maintain network lifetime over 360 days (for most field sizes). It still supports 273 running days for a giant area of 20.8 km² (5 times of the original size). Two types of sensors have shorter lifetime but still much longer than the single type. The difference among "Solar+Wireless," "Wind+Wireless" and "Wireless" becomes smaller when the area increases. This is because, relying on a single energy source is unstable when it suddenly becomes unavailable, that is more likely for larger field sizes. The lifetime of single energy harvesting sensor is the worst, which lasts for only about 20 days even for small

area of 1.1km². Our framework achieves at least 3 times longer lifetime compared with traditional network of a single energy source. Meanwhile, the network depending on solar energy usually enjoys longer lifetime, since energy density of solar radiation is larger and the radiation is more consistent than wind. It is also observed that combining more than 2 types of energy harvesting sensors with the wireless ones is more beneficial for extending network lifetime.

B. Energy Output and Traveling Cost of MC

In this subsection, we evaluate network energy status using different methods to deploy EHBS and the number of EHBS needed to satisfy the energy demands of MC. Fig. 6 (a) demonstrates the total residual energy of q EHBS for different deploying strategies. The residual energy is the average energy remaining of the q EHBS over 360 days. It is difference of the harvested energy and the energy dissipated to replenish the MCs. One MC is assigned to one EHBS and responsible for the charging of one region.

Fig. 6 compares a few possible strategies of deploying EHBS. "Joint" is proposed in Section IV. "Max Energy" deploys EHBS at the position with the maximum energy. "Min Travel" deploys EHBS at the centroid of each region. "Random" deploys q EHBS randomly in the field following a uniform distribution. We can see that residual energy grows with an increasing number of EHBS for all cases. For all four q values, "Joint" always has the maximum energy storage while "Random" is the worst. For $q = 5, 7$, the residual energy of "Min Travel" and "Random" is less than 0. When q is small, it is more important to wisely pick the locations of EHBS, since one false deployed EHBS is less likely to be compensated by other EHBS. "Max Energy" is always better than "Min Travel" since the harvested energy is much larger. The difference between the strategies becomes less obvious when q increases, because reduced region size weakened the impact from location choices.

Fig. 6 (b) shows the relation between the minimal number of EHBS needed to maintain energy balance. For a field of certain area, the minimal number of EHBS needed to maintain energy balance is evaluated for different deploying strategies. Maintaining energy balance needs to ensure the continuous operation. It shows that the minimal number of EHBS for "Joint" increases almost linearly with the increase of field size. The number for "Max Energy" is larger than "Joint" but still linear. "Min Travel" and "Random" increase much

faster. "Random" grows the fastest. This is because random deployment tends to leave coverage holes for some regions and cause network disruption.

C. Network Coverage and Charging Capability

Finally, we evaluate network coverage and charging capability of an MC by comparing with the previous work that charges all sensors in [20]. Fig. 7 (a) demonstrates coverage percentage with the number of MCs in terms of grids. The coverage percentage is the ratio of grids covered by MC to the total number of grids. "Max Cover" applies the maximum coverage charging algorithm. It jointly schedules the activities of charging sensors and replenishing the energy of MC for the maximum coverage rate of different grids. "All Cover" is the previous approach in [20], which fulfills all charging requests in one grid first before moving to the next one. It is observed that our algorithm exhibits significant improvement for the coverage percentage of grids. "Max Cover" achieves 100% coverage ratio while "All Cover" achieves at most 58%. The coverage ratio increases for our algorithm when the number of EHBS increases, since larger q means less traveling cost for MC to replenish its own energy and also smaller size of grids. "Max Cover" does not achieve 100% sometimes with a few MCs, because of large energy request number vs. charging capability.

Fig. 7 (b) shows the covering capability of one MC for different charging algorithms. Covering capability is represented by the largest area one MC can serve (timely response to all the requests). As shown in Fig. 7 (b), the proposed "Max Cover" algorithm yields over 2 times charging capability for one MC than the "All Cover" algorithm, i.e., the charging capability is doubled. The charging area is not affected much by the increase of the grid size whereas it is not the case for "All Cover." This is because larger grid means more sensors to be charged in one grid if "All Cover" is applied. This would then postpone charging in other grids. When q increases, both algorithms have larger covering area because more EHBS means shorter traveling distance for the MC, therefore it can spend more time in charge as well as enlarge its covering area.

VII. Conclusions

In this paper, we propose a new self-sustained WSN via integrating multi-source energy harvesting with wireless charging. First, we derive the optimal composition of different types of sensors by solving a maximum flow problem to minimize manufacturing cost. Second, we jointly consider both energy distribution and moving cost to deploy EHBS. Finally, we propose a scheduling algorithm for the MC to coordinate wireless charging and energy replenishment at EHBS, prove its NP-hardness and propose a 3-approximation algorithm. Finally, we demonstrate that the framework significantly extends network lifetime and improves energy efficiency through extensive simulations.

References

[1] S. Guo, L. He, Y. Gu, B. Jiang, and T. He, "Opportunistic flooding in low-duty-cycle wireless sensor networks with unreliable links", *IEEE Transactions on Computers (TOC)*, 2014.

[2] L. Tang, Y. Sun, O. Gurewitz, and D.B. Johnson, "PW-MAC: An energy-efficient predictive-wakeup MAC protocol for wireless sensor networks", *IEEE INFOCOM*, 2011.

[3] W. Xu, W. Liang, X. Jia, Z. Xu, Z. Li, and Y. Liu, "Maximizing sensor lifetime with the minimal service cost of a mobile charger in wireless sensor networks", *IEEE Transactions on Mobile Computing (TMC)*, 2018.

[4] K. Solangi, M. Islam, R. Saidur, N. Rahim, and H. Fayaz, "A review on global solar energy policy", *Renewable and Sustainable Energy Reviews*, 2011.

[5] M. Magno, S. Marinkovic, D. Brunelli, E. Popovici, B. O'Flynn, and L. Benini, "Smart power unit with ultra low power radio trigger capabilities for wireless sensor networks", *IEEE DATE*, 2012.

[6] B. Kellogg, A. Parks, S. Gollakota, J. Smith, and D. Wetherall, "Wi-Fi backscatter: Internet connectivity for RF-powered devices", *ACM SIGCOMM*, 2014.

[7] J. Bernal-Agustn, and R. Dufo-Lpez, "Simulation and optimization of stand-alone hybrid renewable energy systems", *Renewable and Sustainable Energy Reviews*, 2009.

[8] S. Nikoletseas, T.P. Raptis, and C. Raptopoulos, "Low radiation efficient wireless energy transfer in wireless distributed systems", *IEEE ICDCS*, 2015.

[9] S. He, J. Chen, F. Jiang, D. Yau, G. Xing, and Y. Sun. "Energy provisioning in wireless rechargeable sensor networks", *IEEE Transactions on Mobile Computing (TMC)*, 2013.

[10] P. Zhou, C. Wang, and Y. Yang, "Leveraging Target k-Coverage in Wireless Rechargeable Sensor Networks", *IEEE ICDCS*, 2017.

[11] Y. Zeng, P. Zhou, J. Liu, and Y. Yang, "A Stackelberg Game Framework for Mobile Data Gathering in Leasing Residential Sensor Networks", *IEEE IWQoS*, 2018.

[12] S. Lin, F. Miao, J. Zhang, G. Zhou, L. Gu, T. He, J. Stankovic, S. Son, and G. Pappas. "ATPC: adaptive transmission power control for wireless sensor networks", *ACM Transactions on Sensor Networks (TOSN)*, 2016.

[13] P. Zhou, C. Wang, and Y. Yang, "Static and Mobile Target k-Coverage in Wireless Rechargeable Sensor Networks", *IEEE Transactions on Mobile Computing (TMC)*, 2018.

[14] C. Wang, J. Li, Y. Yang and F. Ye, "A hybrid framework combining solar energy harvesting and wireless charging for wireless sensor networks", *IEEE INFOCOM*, 2016.

[15] F. Akhtar, M. Rehmani, "Energy replenishment using renewable and traditional energy resources for sustainable wireless sensor networks: A review", *Renewable and Sustainable Energy Reviews*, 2015.

[16] RAV Power Solar Charger, Vevor Wind Trubine, and Cubevit Wireless Charger, "http://www.amazon.com".

[17] V. Khare, S. Nema, and P. Baredar. "Solar–wind hybrid renewable energy system: A review", *Renewable and Sustainable Energy Reviews*, 2016.

[18] A. Fahrenbruch and B.R. Bube, *Fundamentals of solar cells: photovoltaic solar energy conversion, Elsevier*, 2012.

[19] G. Cicia, C. Luigi, D. Teresa, and A. Palladino, "Fossil energy versus nuclear, wind, solar and agricultural biomass: Insights from an Italian national survey", *Energy Policy*, 2012.

[20] C. Wang, S. Guo, and Y. Yang, "An optimization framework for mobile data collection in energy-harvesting wireless sensor networks", *IEEE Transactions on Mobile Computing (TMC)*, 2016.

[21] V. Malhotra, M. Kumar, and S. Maheshwari. "An $O(|V|^3)$ algorithm for finding maximum flows in networks", *Information Processing Letters*, 1978.

[22] H. Song, "A method of mobile base station placement for High Altitude Platform based network with geographical clustering of mobile ground nodes", *Computer Science and Information Technology*, 2008.

[23] R. Van, M. Matthias, R. Niedermeier, and M. Weller, "Interval scheduling and colorful independent sets", *Journal of Scheduling 18*, 2015.

[24] C. Papadimitriou, and K. Steiglitz, *Combinatorial Optimization : Algorithms and Complexity, Dover*, 1998.

[25] F. Spieksma, "On the approximability of an interval scheduling problem", *Journal of Scheduling 2*, 1999.

[26] B. Gaudette, H. Vinay, V. Sarma, and K. Marwan, "Optimal range assignment in solar powered active wireless sensor networks", *IEEE INFOCOM*, 2012.

[27] Solargis, "http://http://solargis.com/".

[28] National Renewable Energy Laboratory, "http://www.nrel.gov".